Stimuli-Responsive Amphiphilic Shells of Kinetically Frozen Polymeric Micelles in Aqueous Media: Monte Carlo Simulations and Comparison to Self-Consistent Field Calculations

Filip Uhlík,* Karel Jelínek, Zuzana Limpouchová, and Karel Procházka*

Department of Physical and Macromolecular Chemistry and Laboratory of Specialty Polymers, Charles University in Prague, Faculty of Science, Albertov 6, 128 43 Praha 2, Czech Republic

Received July 27, 2007; Revised Manuscript Received January 29, 2008

ABSTRACT: The behavior of amphiphilic shells of micelles with kinetically frozen hydrophobic cores in aqueous solutions was studied by Monte Carlo (MC) simulations. The calculations emulate the behavior of water-soluble shell-forming chains containing a relatively low fraction of strongly hydrophobic units, which are arranged in either sequences or are distributed uniformly in shell-forming chains. The analysis of concentration profiles of individual species reveals strong segregation and important self-organization of hydrophobic units in the shell. In this paper, we present new MC data. Further, we compare MC and self-consistent field (SCF) results and analyze possible sources of differences. The study shows that the SCF approach is applicable for studied systems, but an unambiguous interpretation of SCF data requires additional information. MC simulations yield detailed and self-explanatory characterization of the shell structure, but they are very time-consuming. The angularly averaged results of both techniques compare reasonably well at the semiquantitative level, but SCF overestimates the pH effects in annealed polyelectrolyte systems. A combination of both methods increases the impact of the study.

Introduction

Polymeric micelles in aqueous media are interesting and practically important self-assembled nanoparticles. Various water-soluble micelle-like structures, mainly stimuli-responsive block polyelectrolyte systems, the properties of which can be controlled by pH and ionic strength, have been studied as external-stimuli-controllable drug carriers in processes of targeted drug delivery, etc.[1,2] A number of research groups have been studying the micellization of block copolymers in aqueous media by different experimental,[3–13] theoretical, and computer-based techniques[14–21] for almost 2 decades. In the past few years, we studied the structure of shells and conformations of shell-forming chains in micelles with kinetically frozen cores experimentally,[22,23] by self-consistent field (SCF)[24–26] and Monte Carlo (MC) simulations.[27,29] Some time ago, we started a systematical study of the conformational behavior of shells formed by polyelectrolyte copolymers with a low fraction of hydrophobic units. Thus far, we investigated mainly the fluorescently end-tagged chains.[23] Recently, we addressed more complex systems. Experimental studies are in progress, and their results will be published in the near future. Nevertheless, their behavior in aqueous media can be reasonably predicted by computer simulations. The first results of the SCF study have been already published.[26] Here we present new MC data and compare MC and SCF predictions.

The aim of the paper is manifold: (i) At first, we present new MC data that show details of the conformational behavior of the shell-forming chains. (ii) We also show that the detailed MC description provides a clue how to interpret the angularly averaged SCF data. (iii) Finally, we analyze common features and differences between MC and SCF approaches. The study is not aimed at the best quantitative agreement of results of both techniques but at the identification, understanding, and explanation of important sources of discrepancies.

* To whom correspondence should be addressed. E-mail: uhlik@sals.natur.cuni.cz (F.U.); prochaz@vivien.natur.cuni.cz (K.P.).

Materials and Methods

Studied System. The synthesis of copolymer samples with segmented polyelectrolyte blocks is in progress, and results of their self-assembling behavior will be reported in the near future. Nevertheless, we are able to predict the behavior in aqueous media by SCF and MC methods. For the modeling, we assume that studied micelles are similar to micelles with homogeneous blocks of the same length that we recently studied by light scattering and other techniques. Hence, we use parameters for kinetically frozen self-assembled spherical nanoparticles formed by polystyrene-*block*-(polymethacrylic acid) with comparably long blocks (ca. 30 000)[22–25] employed recently in our computer studies of PS−PMA micelles.[27,28] The frozen core is modeled as a hydrophobic sphere to which the shell-forming chains are tethered and the shell is modeled as a spherical polymeric brush. The shell-forming block is an amphiphilic chain containing a high content of an annealed polyelectrolyte (E) and a relatively low fraction (10 or 20%) of strongly hydrophobic units (H). The H units are distributed either uniformly or are arranged in one or two short sequences inside the hydrophilic chain (see Figure 1). The same value of the dissociation constant for monomeric methacrylic acid, $pK_a = 4.69$, was used as in our earlier studies.[26–28] We study very dilute solutions, and therefore, we consider one micelle immersed in the solvent only. Because the core-forming chains are long, the H sequences are short, and all properties of polymers (e.g., solubility or glass transition temperature, T_g) depend upon the length of the chain or its distinct chemical parts (in the case of block of graft copolymers, where two different T_g values can be detected), we assume that the cores are kinetically frozen but the domains are in a reversible (mobile) equilibrium.

The directly experiment-derived parameters are association number, $N_{AS} = 113$, and core radius, $R_C = 12$ nm.[22,23] The association number was actually obtained on the basis of empirical scaling relations published by Quin et al.[30] (for a 1,4-dioxane (80%)−water mixture) for a PS−PMA sample studied recently.[31] The size of the spherical core was recalculated from the association number using the density of bulk polystyrene, 1.05 g/cm^3.[32] Other parameters were obtained indirectly by the mapping procedure aimed at reproducing the most important structural features of the real system by the coarse-grained model (ratio of the contour length of shell-forming chains to the radius of the core and the flexibility

10.1021/ma071675q CCC: $40.75
Published on Web 04/25/2008

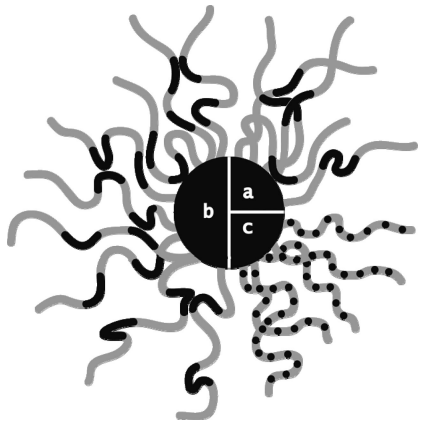

Figure 1. Schematic depiction of studied systems with (a) one hydrophobic sequence, (b) two sequences, and (c) an alternating copolymer. Weak polyelectrolyte units are shown in gray, and hydrophobic units and the core are shown in black.

Table 1. SCF Flory−Huggins Interaction Parameters χ and MC Interaction Energies ε[a]

χ	E	H	S	ε/kT	E	H
E	0.0	0.0	0.5	E	0.8	0.6
H		0.0	5.0	H		−3.0
S			0.0			

[a] E stands for polyelectrolyte; H stands for hydrophobic units and the core; and S stands for solvent.

of real chains, i.e., the characteristics ratio C_∞, which reflects the effect of bond-angle restrictions and rotational barriers in real chain). The indirectly derived parameters are the lattice constant, $l = 1$ nm, and the number of the Kuhn segments, $N = 100$. The coarse-graining and back-mapping procedure is a delicate task and was described and discussed in detail in our earlier studies.[23–25,27]

The parameters describing the short-range van der Waals interactions have been optimized in our earlier studies and are given in Table 1. They model a system in which the solvent is an effective θ solvent for the nonionized E units and a very strong precipitant for the core and hydrophobic units (we assume the same value for the core−solvent and H−solvent interaction). In both MC and SCF, the concentrations of H_2O, H_3O^+, OH^-, and small ions Na^+ and Cl^- control bulk pH and ionic strength, but with regard to short-range van der Waals interactions, the solvent is treated as one component. Its role is accounted for only implicitly, which means that the algorithm focuses on polymer chains and the solvent is assumed to occupy the lattice sites that are not occupied by the units of the polymer chain. The contribution of electrostatic forces is added to the energy that is taken into account during the optimization of the system behavior.

MC Simulation. We have been using MC simulations on a simple cubic lattice. The shell-forming chains are tethered to the micellar core, which is located in the center of the simulation box. The chains are modeled as the fully inter- and intrachain self-avoiding walks. We employ two basic moves for the equilibration of the system: (i) dissolution and random growth of a random part of a random chain and (ii) dissolution and random growth of a randomly chosen chain from a new randomly selected position at the core surface. The electrostatic contribution is treated indirectly by solving the radial Poisson–Boltzmann (PB) equation. A standard Metropolis acceptance/rejection criterion takes into account the short-range interactions (reflecting the selectivity of the solvent and the compatibility of individual polymeric units) and the long-range electrostatic forces. Details of the simulation method were described in our earlier paper.[27]

SCF Calculations. The studied micelles are on average spherical nanoparticles, and therefore, we perform simulations on a spherical lattice with the origin in the center of the spherical core. Using the radial self-consistent-field method developed by Scheutjens and Fleer,[33] we model the micellar shell as a brush tethered to the hydrophobic spherical core. The fundamentals of this method for neutral chains, as well as for annealed polyelectrolytes and the pertinent computational schemes, were described in a number of papers.[33–35] Results of SCF calculations have already been published,[26] but because we compare MC and SCF results, basic information on the used SCF has been included.

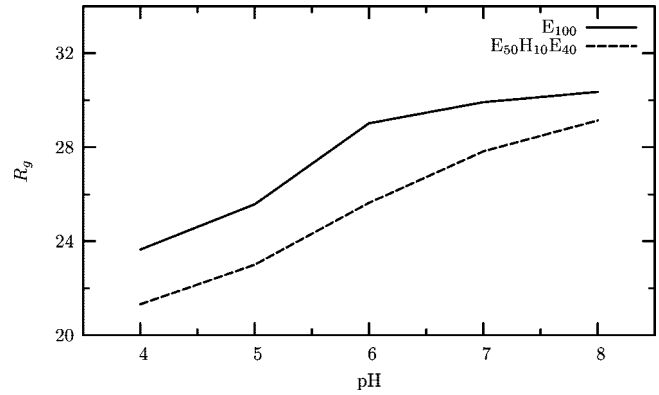

Figure 2. Simulated dependence of R_g on pH for $I = 0.01$. The standard deviation is ca. 1 nm.

Results and Discussion

The main goals of the paper are (i) detailed study of nanoheterogeneous micellar shells by the MC method and (ii) critical comparison of MC and SCF results. As already mentioned, we do not try to achieve good quantitative agreement of SCF and MC results at any cost. We try to identify and analyze the most important sources of discrepancies (mainly those imposed by the SCF symmetry assumption). However, for any meaningful comparison, a careful setting of mutually corresponding parameters of the model system is necessary as it was stressed by several authors,[36–46] who compared MC and SCF results for different systems. To obtain mutually corresponding parameters, we used the strategy similar to that described by Leermakers,[38] but χ parameters for E units were not just recalculated from pertinent ε parameters and corrected for different numbers of neighbors taken into account in both lattice models. They were optimized to obtain the same size for generic PS−PMA micelles at low pH, where the electrostatics plays a negligible role. The incompatibility of E and H units is modeled indirectly via attractive HH interactions. The ε_{HS} and χ_{HS} parameters model an extremely bad solvent for H units; however, one fact have to be clearly stated: Because the SCF results do not change with the worsening χ_{HS} parameter beyond 5 but the numerical solution slows down considerably, we used $\chi_{HS} = 5$, which allows for reasonably fast calculations and corresponds to a strong precipitant for H units, anyway.

MC Simulations. In this paper, we study several types of micellar systems with hydrophobically modified shell-forming blocks. The used MC variant strongly alleviates the symmetry burden. The simulations provide detailed information on the shell structure, and we focus mainly on differences between modified and generic systems. Nevertheless, in the beginning of this paragraph, we present dependences of averaged characteristics that can be measured experimentally (as suggested by the referee) for a system with one H sequence close to the middle of the shell-forming chain, i.e., for a system that can, according to our opinion, find interesting applications in targeted drug delivery and in complex systems formed on the basis of hierarchy principles of the bottom−up self-assembly into larger structures. Because the benchmark technique for the characterization of micelles is the static light scattering, in Figure 2, we show dependences of R_g on pH for the generic system E_{100} and $E_{50}H_{10}E_{40}$ (for $I = 0.01$). The effect of pH and ionic strength

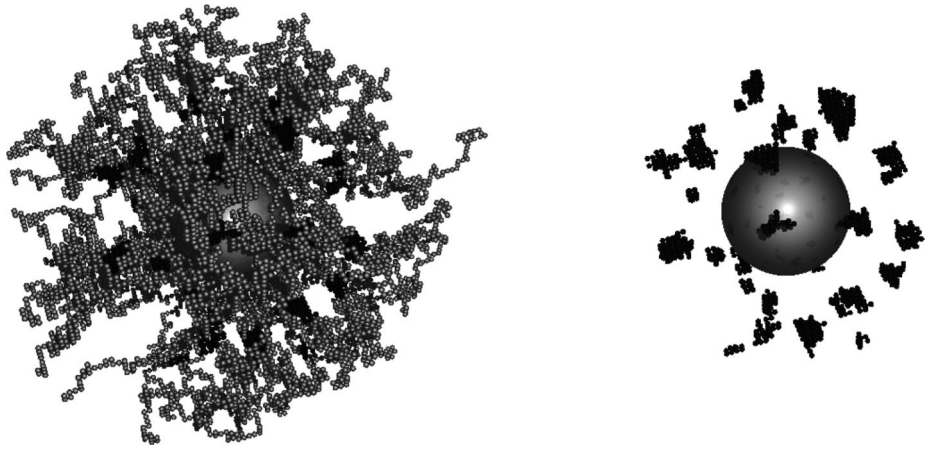

Figure 3. Snapshot of the $E_{30}H_{10}E_{60}$ system for pH 7 and $I = 0.01$. Polyelectrolyte units and the core are light gray, and hydrophobic units are dark gray. Hydrophobic beads alone are shown on the right.

on weak polyelectrolyte shells has been studied by a number of research teams[3–28] and is well-known and understood. In the studied pH range, the used MC variant yields the rising part of sigmoidal R_g versus pH dependences. We focused on this pH region only because both experimental and our earlier MC and SCF studies show that, outside this region, the R_g values are almost constant.[27] The R_g versus pH plots reveal slight differences in the overall shell stretching because of hydrophobic modification. Despite the complex shell structure of modified systems, the decrease in the shell stretching with respect to the generic system is small. This finding is not surprising, because the same effect was observed in our earlier SCF study of analogous systems.[26,28] It is at least an important message for experimentalists that not all systems that appear as simple core/shell micelles and fulfill some assumed dependences have to be simple micelles and have to obey all principles of the assumed behavior. In comparison to SCF, the MC-predicted shell expansion is rather small. We point out that this finding was also expected because we found similar differences between MC and SCF results in our earlier studies.[22,23,28] Their origin will be discussed in detail in the Comparison of MC and SCF Data section.

With regard to the experimental studies, larger differences between modified and generic systems could be expected in scattering functions (form factors) measured by small-angle neutron scattering (SANS) for selectively deuterized samples. Because we use the lattice MC simulation, the simulated scattering functions are affected by the periodicity of the lattice, particularly in the q range, where differences because of the presence of fairly small domains can be expected. It is why the simulated form factors do not provide useful information.

In the next part, we will focus on the behavior of systems with 10% of H units arranged in one block "moving" along the contour of the shell-forming chain: $E_{30}H_{10}E_{60}$, $E_{50}H_{10}E_{40}$, and $E_{90}H_{10}$.

MC simulations provide (i) ensemble average characteristics and their distributions and (ii) simulations snapshots. The former are relevant statistical averages and provide reliable characterization of the equilibrium behavior of the system under investigation. The snapshots show selected (more or less probable) instantaneous system configurations (in our case shell structures) and conclusions based on snapshots only can be by far misleading. However, a careful inspection of a statistically relevant number of snapshots and correct identification and selection of a "typical structure" (which "complies with" all ensemble average characteristics) can help to understand the behavior in detail and simplify the discussion.

To give readers an idea on the structure of studied systems, we first show typical snapshots of three systems: $E_{30}H_{10}E_{60}$, $E_{90}H_{10}$, and an alternating system with the same content of H units $(E_9H)_{10}$ as the previous two (for comparison as a reference system), in solutions with pH 7 and $I = 0.01$, and describe them.

The left of Figure 3 depicts a snapshot of the $E_{30}H_{10}E_{60}$ system at pH 7 and $I = 0.01$. Polyelectrolyte units and the core are represented by the light gray color, and hydrophobic units are represented by the dark gray color. In the right of Figure 3, only the core and hydrophobic units are shown to yield as comprehensive of a picture as possible. The snapshot shows a relatively expanded polyelectrolyte shell (a fairly high fraction of E units are ionized at pH 7 for a system with assumed pK_a) with a number of distinct H domains. An important fraction of H domains are located quite far from the core, but some chains collapse or recoil. H sequences return back close to the core and form H domains adsorbed on the core. The snapshot immediately reveals the most obvious feature of the conformation behavior: (i) strong inhomogeneity of the shell and (ii) spontaneous self-organization of insoluble H units in hydrophobic domains. Figure 4 shows the snapshot of $E_{90}H_{10}$ system with the H block at the free end of the shell-forming chain. In this case, an important number of hydrophobic domains form quite far from the core. The domains in the dilute part of the shell are relatively small (they are quite often collapsed H sequences of one chain only), and their number is higher than that in the previous case; however, the fraction of domains in the immediate vicinity of the core (adsorbed at it) is also important. It means that a non-negligible fraction of end-modified chains either collapse or form loops. In one of our earlier studies on fluorescently end-tagged systems[29] (containing strongly hydrophobic fluorophores), we have shown that the loop formation can be almost excluded in end-modified systems and that some tagged chains collapse while others expand (see, e.g., the 2D distribution function in Figure 5 in ref 29). Because both systems are similar with regard to interactions with the solvent, we assume that the same type of behavior applies also in the studied system. The above assumption is supported by the fact that the snapshot shows a fairly dense inner shell from which only few stretched chains reach the shell periphery. The third snapshot (Figure 5) depicts the structure of the shell formed by chains with a uniform distribution of H units, i.e., $(E_9H)_{10}$. The figure suggests that all chains are more or less uniformly expanded and that H units are randomly distributed without any sign of domain formation.

To support the relevance and general validity of the above observations, in the next part, we analyze the shapes of the

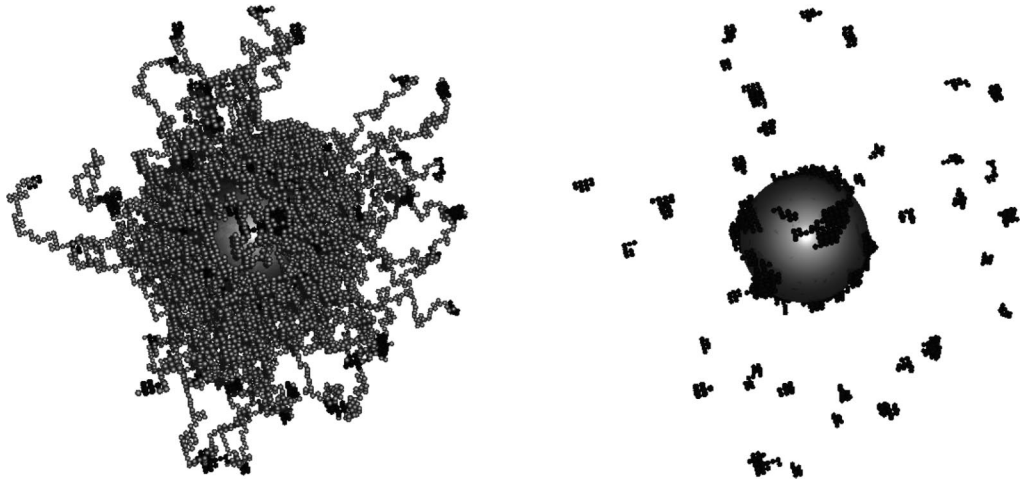

Figure 4. Snapshot of the $E_{90}H_{10}$ system for pH 7 and $I = 0.01$. Polyelectrolyte units and the core are light gray, and hydrophobic units are dark gray. Hydrophobic beads alone are shown on the right.

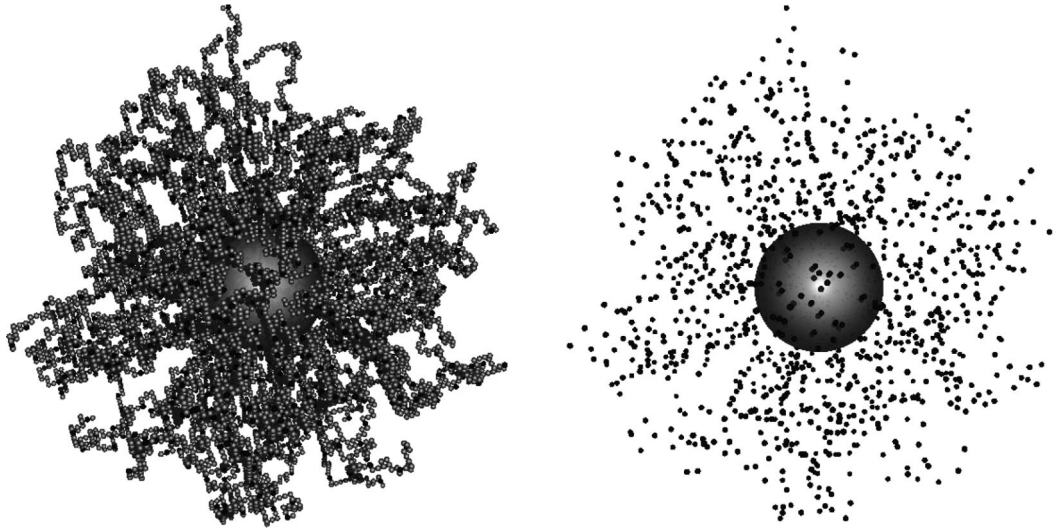

Figure 5. Snapshot of the $(E_9H)_{10}$ system for pH 7 and $I = 0.01$. Polyelectrolyte units and the core are light gray, and hydrophobic units are dark gray. Hydrophobic beads alone are shown on the right.

ensemble average radial concentration profiles of the shell. For further discussion, we define hydrophobic domains as areas with appreciably increased concentration of H units (with respect to the rest of the shell). These domains still contain solvent molecules and possibly some E units. In Figure 6, we present the probability density functions $\pi_i(r)$ of finding a shell-forming bead of type i at a specified distance r from the core center for pH 5 and $I = 0.01$, for systems $E_{30}H_{10}E_{60}$, $E_{50}H_{10}E_{40}$, $E_{90}H_{10}$, $(E_9H_1)_{10}$, and E_{100}. The functions $\pi_i(r)$ are normalized by the following formula: $\int_{r=R_C}^{R_{max}} \pi_i(r)dr = 4\pi \int_{r=R_C}^{R_{max}} \rho_i(r) r^2 dr = 1$, where $\rho_i(r)$ are number densities of pertinent monomer units. From Figure 6, it is evident that the probability densities of finding any bead in the distance r, $\pi_{tot}(r)$, do not differ much in systems E_{100} and $(E_9H)_{10}$. The distribution of H units in the latter system, i.e., the probability density of finding a hydrophobic bead in a distance r, $\pi_H(r)$, is very broad and uniform, confirming that H domains do not exist in this system, which is in agreement with corresponding snapshots.

Probability densities $\pi_{tot}(r)$ and $\pi_H(r)$ in systems with a single sequence of H units differ significantly from those for the alternating system. The results of a series of simulations for systems with the H sequence at different positions can be summarized as follows: The H units in a system with a single hydrophobic sequence relatively close to the core-tethered end of the chain tend to adsorb at the core. With the sequence

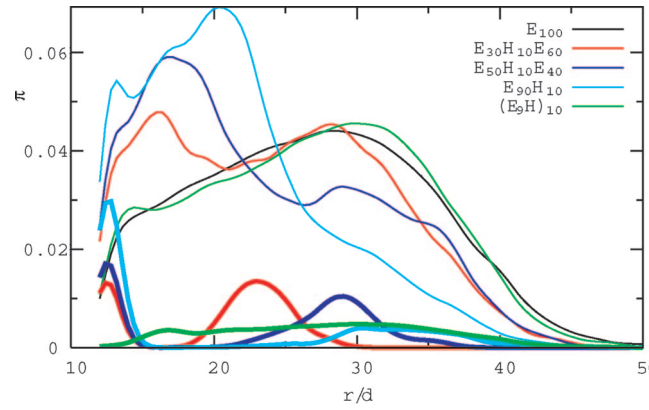

Figure 6. Probability density functions of finding a bead, any one (upper thin curves) and the hydrophobic only (lower bold curves), at a distance from the core center r for pH 5 and $I = 0.01$ (the integrated area below π_{tot} curve equals 1, and that below π_H equals 0.1).

position "moving" from the core−shell interface (i.e., along the contour of the shell-forming chain to the shell periphery), a close approach of hydrophobic units to the core becomes less favorable from the entropy point of view and the hydrophobic sequences start to form hydrophobic domains far from the core.

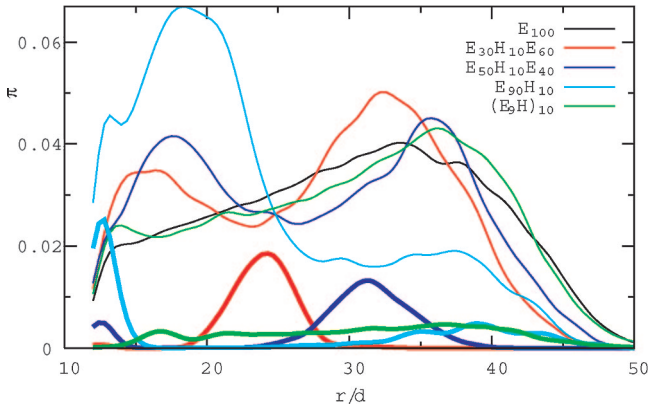

Figure 7. Same curves as in Figure 6 but for pH 7.

The distance from the core increases with the sequence offset, and the domains are distributed in a broader r range. Some chains collapse, and their H sequences come to the immediate vicinity of the core, as witnessed by the increased probability of finding hydrophobic units near the core. Other chains remain fairly stretched, which translates in the shoulder on density profiles at large distances. The H sequences in stretched chains self-assemble and form relatively small H domains. At fairly large distances, the formation of hydrophobic domains is further hindered as the space opens up and the shell dilutes. Nevertheless, even in the limiting $E_{90}H_{10}$ system, some H sequences self-assemble and form domains at the dilute shell periphery and a significant fraction of H units in collapsed chains form the core-adsorbed hydrophobic domains (from pertinent snapshots, we can deduce that the coverage of the core is not uniform but individual well-segregated domains adsorb separately on the core). The shape of the probability density $\pi_{tot}(r)$ with a pronounced maximum at lower r (as compared to all other systems) indicates that an important fraction of shell-forming chains are collapsed and that only a limited number of stretched chains reach the shell periphery.

Figure 7 depicts the probability density functions $\pi_i(r)$ for the same systems as in the previous figure at pH 7 and $I = 0.01$. It is immediately evident that an increased ionization (and hence stronger electrostatic repulsion) promotes the expansion of the shell and supports the formation of H domains further from the core in systems with the H sequence close to the middle of the shell-forming chains. It is interesting that the stretching of noncollapsed chains in the $E_{90}H_{10}$ system increases with pH, but the electrostatic repulsion does not prevent the collapse and adsorption of an important fraction of H units. Besides the pronounced increase in the shell thickness, the role of pH on the inner structure of the shell can be characterized as follows: Increasing pH promotes the conformational transition from the regime with the core-adsorbed H domains to the regime with well-segregated domains far from the core. For almost all systems, there exists a coexistence region of several pH units depending upon the position of the H sequence, where the core-adsorbed and fairly stretched domain-forming chains coexists in equilibrium; i.e., the functions describing composition of the shell are bimodal.

Increasing ionic strength generally screens electrostatic interactions and weakens the effect of pH. The density functions for two hydrophobically modified systems $E_{50}H_{10}E_{40}$ and $(E_9H)_{10}$ at pH 7 and four values of ionic strength $I = 0.001$, 0.01, 0.1, and 1 are depicted in Figures 8 and 9. In sequenced systems, the H domains exist in a broad range of ionic strengths, but as the electrostatic repulsion becomes screened at high I, they shift closer to the core and the fraction of core-adsorbed H units increases. In the case of alternating systems, the behavior

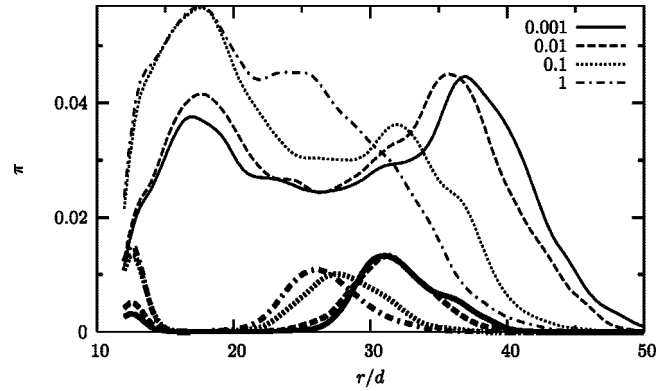

Figure 8. Probability density functions of finding a bead, any one (upper thin curves) and the hydrophobic only (lower bold curves), at a distance from the core center r for $E_{50}H_{10}E_{40}$ at pH 7 and $I = 0.001$, 0.01, 0.1, and 1.

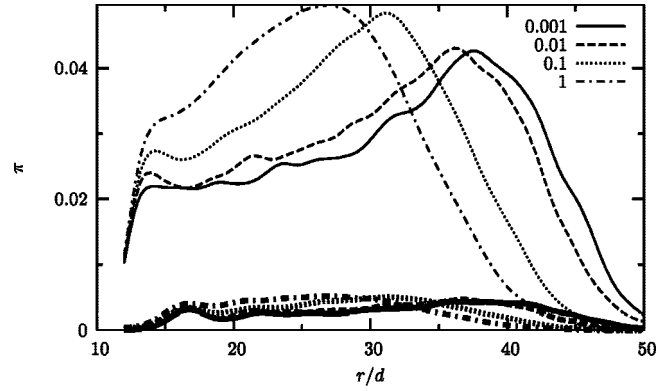

Figure 9. Probability density functions of finding a bead, any one (upper thin curves) and the hydrophobic only (lower bold curves), at a distance from the core center r for $(E_9H)_{10}$ at pH 7 and $I = 0.001$, 0.01, 0.1, and 1.

is simpler and the shell merely shrinks with increasing I, while the hydrophobic units stay always fairly uniformly distributed.

Besides the ensemble average behavior, we also studied the uniformity of equilibrium shells (polydispersity and distribution of domain sizes, etc.), because the distribution and variability of structural properties affects the practical applicability of designed systems. For a detailed characterization of the shell structure, the most desirable would be the 2D function correlating the size of H domains and their position in the shell. Despite the fact that the discernment of areas differing in concentrations of individual units looks like a simple task for a powerful computer, an unambiguous identification of hydrophobic domains and the evaluation of a number of their units is not a trivial problem and requires great care. We use a simple criterion that is based on the identification of continuous areas ("hydrophobic islands") of H units, which have two or more nonbonded lattice neighbors. It is a clearly defined criterion that unambiguously discerns the dense hydrophobic areas from the rest and can be easily employed during simulations. Nevertheless, an explanation of the meaning of the distribution function, which is obtained and will be presented, is needed. In the previous part, we defined H domains as areas with an appreciably increased concentration of H units, which still contain an important amount of the solvent (i.e., they are not kinetically frozen but swollen and can rearrange at measurable real times, even though this aspect is not a part of this study). Figure 10 elucidates the difference between domains defined on the basis of concentrations of individual units and "hydrophobic islands" defined as continuous areas of densely packed H units. It shows a swollen H domain formed by the self-assembly of H sequences

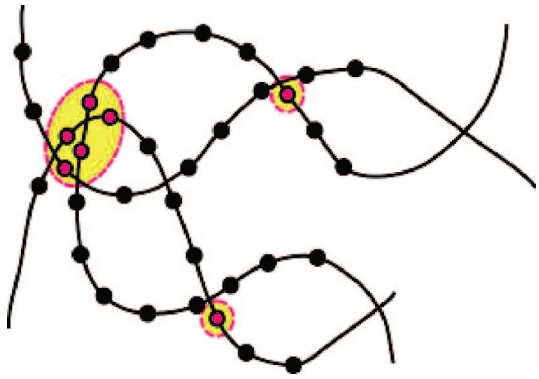

Figure 10. Two-dimensional depiction of the hydrophobic domain formed by three chains. Black circles represent the H units, and red circles represent H units that have two or more nonbonded immediate neighbors. Red ellipses mark hydrophobic islands.

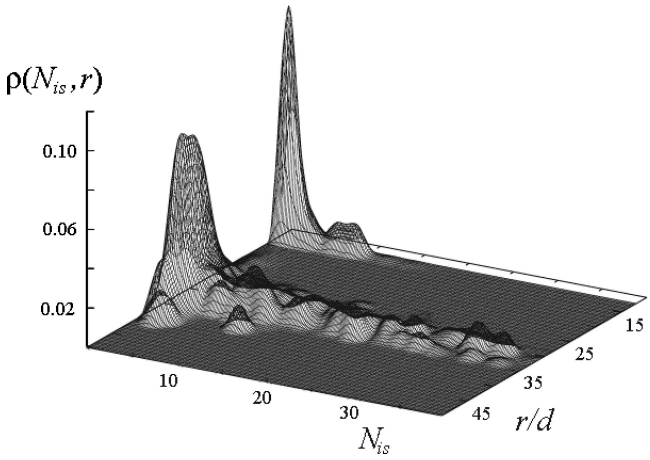

Figure 11. Normalized fraction, $\rho(N_{is},r)$, as function of the number of H units forming the island, N_{is}, and the radial position of their gravity centers, r, for $E_{40}H_{10}E_{50}$ at pH 7 and $I = 0.01$.

from three chains. An inspection reveals that only few H units fulfill the condition of two or more nonbonded immediate neighbors. Further, the depicted domain splits in several continuous hydrophobic islands: one containing five H units and two isolated H units imitating very small isolated islands. We can conclude that the function that we are going to present does not yield the total number of H units in swollen H domains but addresses a bit different physical problem and focuses on the distribution of the most hydrophobic areas (H islands) in the shell. Hence, on one hand, one has to be careful when comparing the 2D distribution with another functions, and on the other hand, the comparison reveals new details, because 1D and 2D functions are aimed at different details of the shell structure.

The normalized fraction, $\rho(N_{is},r)$, of different islands as a function of the number of H units forming the island, N_{is}, and the radial position of their gravity centers in the shell, r, is depicted for $E_{40}H_{10}E_{50}$ at pH 7 and $I = 0.01$ in Figure 11. The accuracy of the evaluation needs one more comment. A reliable evaluation of a 2D distribution function requires very high statistics (to yield the same noise and accuracy when calculating a 2D distribution function, n^2 data points are needed as compared to n points for 1D distribution function). Therefore, we present one example only to give an idea on the distribution of island sizes and their positions. Even though its enumeration required almost 2 months of real time in the computer center (under normal working regime, i.e., without special priorities), the function still shows oscillations.

The shape of the 2D function shows that the hydrophobic islands are localized either close to the core or at a certain constant distance irrespectively of their sizes (punctually of N_{is}). Assuming that the dense islands are localized inside lager hydrophobic domains and combining new pieces of information with those obtained from snapshots and 1D functions, we can interpret the shape of the curve as follows: A sharp maximum at relatively low N_{is} suggests that the H domains are appreciably inhomogeneous and contain several dense hydrophobic islands. Because the islands are small, we can assume that larger domains do not freeze for longer times. This finding is important because the association of H units does not affect the simulation and further supports our basic premise that the core is frozen but the domains are not. The tail toward fairly high N_{is} shows that a small fraction of larger and compact H islands does exist in the shell. It has to be taken into account that a relatively low number fraction of large hydrophobic areas (both islands and swollen domains containing relatively high numbers of H domains) translates in their fairly large weight fraction.

The last part of the MC study was devoted to more complex systems. The motivation for the investigation of complex systems was the following: Experimentally, it is sometimes easier to synthesize irregular multiblock copolymers than well-defined di- or triblocks. Therefore, it is interesting to study the behavior of such systems. We simulated several systems with two H sequences that are sufficiently far away from the core and also from each other. For the sake of brevity, we confine to a detailed discussion of one system only. A typical snapshot for the system $E_{25}H_{10}E_{30}H_{10}E_{25}$ (pH 7, $I = 0.01$) is depicted in Figure 12. Probability density functions $\pi_{tot}(r)$ and $\pi_H(r)$ for pH 5 and 7 and $I = 0.01$ are shown in Figures 13 and 14. The simulation shows that the behavior of shells formed by chains modified by two hydrophobic sequences is similar to that of single modified systems; however, it is more complex. The regions of distances where the hydrophobic domains form are broader as compared to systems containing only one hydrophobic sequence, because units of both sequences from different chains may contribute to the formation of the same domain.

Comparison of SCF and MC Data. The angularly averaged results of MC simulations compare well with those of recently performed SCF calculations[26] at the qualitative level. We can summarize that the same trends of the behavior were obtained by both techniques. Some differences exist at the semiquantative level, and a quantitative agreement is rather poor. For detailed analysis of similarities and differences, we have chosen a system with one H sequence in a relatively narrow region of pH 5–7, because the conformational behavior is very sensitive to pH and ionic strength in this region and differences between MC and SCF are very obvious. Both MC and SCF predict (i) adsorption of H units at the core in systems with short E_1 sequences, (ii) formation of hydrophobic domains far from the core in systems with long E_1 sequences, and (iii) in systems with the H sequence approximately in the middle of the shell-forming chains, the pH- or I-provoked conformational transition from the regime with core-adsorbed H sequences to the domain-forming regime. In Figures 15 and 16, we compare the angularly averaged probability densities of finding any monomer unit, $\pi_{tot}(r)$ and a hydrophobic unit, $\pi_H(r)$, in a distance r from the core for a system with the H sequence in the middle of the shell-forming chain, i.e., for $E_{50}H_{10}E_{40}$ at pH 5 and 7, respectively, for two values of ionic strength, $I =$ (a) 0.01 and (b) 0.1. The comparison is highly instructive. It shows that MC simulations underestimate and that the SCF approach overestimates the role of electrostatic forces. This finding agrees with results of our earlier works devoted to the comparison of computer-based and experimental studies on the pH-controlled behavior of PMA shells.[22,23,28]

A close inspection of individual curves shows that both methods predict a pH- and I-dependent conformational transition

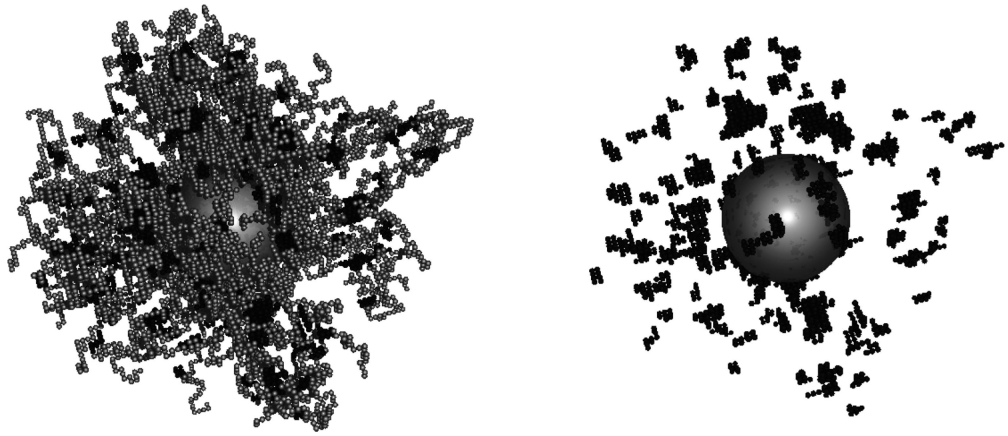

Figure 12. Snapshot of the $E_{25}H_{10}E_{30}H_{10}E_{25}$ system for pH 7 and $I = 0.01$. Polyelectrolyte units and the core are light gray, and hydrophobic units are dark gray. Hydrophobic beads alone are shown on the right.

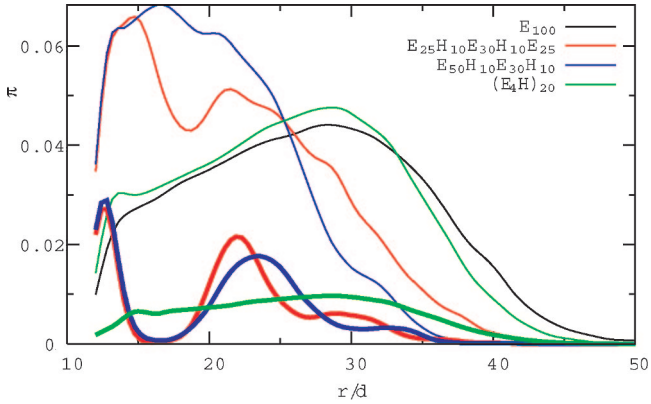

Figure 13. Probability density functions of finding a bead, any one (upper thin curves) and the hydrophobic only (lower bold curves), at a distance from the core center r for pH 5 and $I = 0.01$. (the integrated area below π_{tot} curve equals 1, and that below π_H equals 0.2).

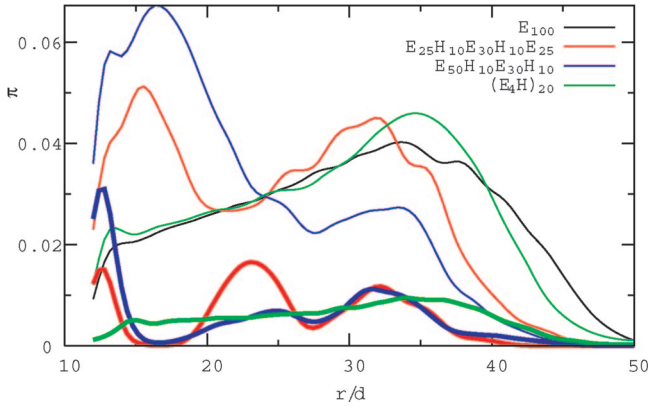

Figure 14. Same curves as in Figure 13 but for pH 7.

from a state with fairly collapsed shell-forming chains and H units adsorbed on the core (at low pH) to a state with fairly stretched chains and distinct hydrophobic domains quite far from the core (at high pH). It is immediately evident that the SCF-predicted stretching is more pronounced and the coexistence region (where both collapsed and stretched chains coexist) is narrower and is shifted to a higher pH as compared to MC.

Details of the shell description (density profiles) provided by SCF and MC also differ. At pH 5, we see that the SCF-predicted density increases steeply in a very narrow r region close to the core (the actual data points are out of scale). The MC curves

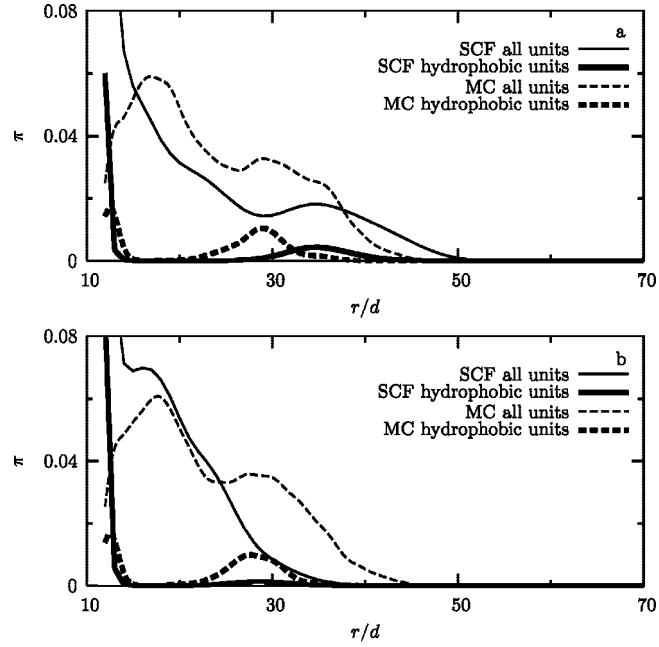

Figure 15. Comparison of MC and SCF probability density functions of finding a bead, any one (upper thin curves) and the hydrophobic only (lower bold curves), at a distance from the core center r for $E_{50}H_{10}E_{40}$ at pH 5 and $I =$ (a) 0.01 and (b) 0.1.

actually drop for small $r \rightarrow 0$. The drop is caused by the well-know entropy effect of the impenetrable core/shell interface.[33]

Before we analyze the most important sources of differences between MC and SCF approaches, possible effects caused by interaction parameters have to be mentioned. The solvent is a θ solvent for un-ionized E chains, and corresponding interaction parameters can be set without problems (approximately the same shell thickness is foreseen by both methods at low pH). However, the hydrophobic nature of H units and the incompatibility of H and E units are described indirectly in SCF via an appropriate combination of Flory–Huggins interaction parameters: strongly repulsive H solvent, weakly repulsive E solvent, and zero H−E parameter, while explicit interaction parameters ε_{EE}, ε_{HH}, and ε_{EH} are employed in MC. The data at low pH suggest that the combination of Flory–Huggins parameters slightly exaggerates the adsorption of H units at the core. Despite the overestimated effect of hydrophobic interactions in SCF, the pH-provoked expansion of E chains overbalances the hydrophobic interactions much faster (i.e., in a narrower pH range) in SCF than in MC calculations. This fact is extremely

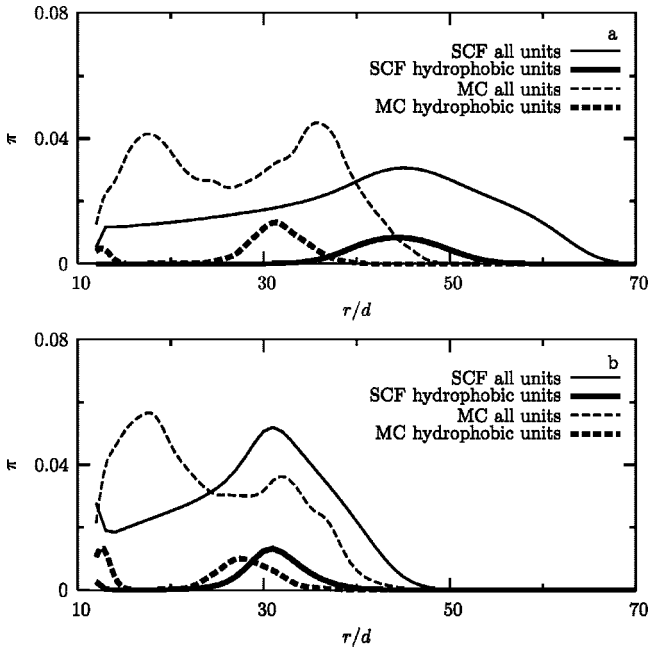

Figure 16. Same curves as in Figure 15 but for pH 7.

important, because it proves that the observed uneven sensitivity of MC and SCF to pH and ionic strength is not caused by inaccurate setting of parameters but is due to different treatments of chains. In MC, all units of all chains are treated explicitly; i.e., the energy of each unit takes into account interactions with all neighbors. The SCF approach treats an average "pseudo-chain" in a mean force field, which corresponds to the average microenvironment (only depending upon the radial position), and hence, it neglects some details of the shell structure. In MC, the interaction potential of the unit under consideration depends upon the arrangement of all surrounding species, while in SCF, it is an effective angularly averaged function of the radial distance from the center of symmetry.

Another important source of differences consists in the fact that the used SCF variant was proposed for "homogeneous" systems (in this case, homogeneous except the radial direction) and *a priori* assumes the spherical symmetry. It surprisingly generates certain inaccuracy and deviation from MC even in systems that obey the spherical symmetry for the following reasons: The applied MC variant employs a simple cubic lattice, and the Metropolis criterion does not prefer any direction during the self-avoiding growth of individual chains. Only the energies of instantaneous configurations are taken into account. In contrast to MC, the radial SCF variant uses a spherical lattice and *a priori* differentiates between radial and tangential directions and treats the properties of chains in different directions in an uneven way (from the structural point of view, the motion in tangential directions is not sufficiently specified).

Both methods handle the self-avoiding character and connectivity of chains differently. While MC simulates the fully connective self-avoiding chains, SCF calculations do respect the self-avoiding character and connectivity of "pseudo-chains" only implicitly. Only the global layer characteristics (e.g., average ratio of occupied to all lattice points) are important and have to obey physical relations during the solution of diffusion-like equations. However, steps in all directions (including a reversal step) are allowed, and the length of the step in a given spherical layer (i.e., perpendicular to the radial direction) is not actually defined. In other words, the equivalence of all lattice points in each layer perturbs the connectivity of "pseudo-chains" in tangential directions. Inequality of radial and tangential directions translates further in a suppression of the excluded volume effect, which is accounted for by the average layer density only. In summary, the SCF "pseudo-chains" are not strictly self-avoiding, not fully connective, and effectively more flexible than the MC chains.

A lower sensitivity of MC than SCF to pH and ionic strength, which we have shown is a result of the different treatment of the self-avoiding character and connectivity of shell-forming chains, is further amplified in systems of annealed polyelectrolytes because electric charges are "mobile". In our MC variant, the self-avoiding character of chains is the "highest imperative" of the conformational behavior. Therefore, many conformations (with energetically favorable instantaneous distributions of charges) are forbidden, and charges on the chain have to redistribute to minimize the electrostatic energy. Thus, in MC, the effect of electrostatic forces (and hence the effect of pH) is rather weak and indirect. An analogous feedback does not exist in SCF and does not attenuate the effect of pH on SCF data. Further, we believe that the high effective flexibility of SCF intersecting "pseudo-chains" contributes also to the observed exaggerated sensitivity of SCF results to pH and *I*.

Conclusions

The performed MC simulations provide a detailed description of the behavior of nanoheterogeneous shells. The obtained results are self-explanatory and reveal the complexity of the conformational behavior of sequenced shell-forming polyelectrolyte chains. The study of shells formed by annealed sequenced shell-forming chains (containing a sequence of 10% hydrophobic units) predicts a pH-controlled conformation transition from a low pH regime, where an important fraction of chains collapses and H units form domains adsorbed on the core to a high pH regime, where H units of fairly stretched chains self-assemble in domains located quite far from the core. The transition is gradual, and there exists a pH region (depending upon the position of the hydrophobic sequence in the chain, ionic strength, etc.) where both conformations coexist in equilibrium and corresponding distribution functions are bimodal.

An important result of the MC study is a piece of information that H domains are localized in relatively narrow spherical layers fairly uniformly. This finding justifies the applicability of the spherically symmetrical SCF and proves that its results are not invalidated because of a major "symmetry collapse".

The comparison of MC and SCF indicates that the latter approach provides only a simplified description of the system behavior. The angularly averaged radial functions compare well at the semiquantitative level, but despite a considerable effort in the optimization of parameters, we did not reach a good quantitative agreement between MC and SCF results. In this respect, our conclusions agree with our earlier observations and those of many other authors. The study shows that a combination of both methods is very useful. SCF is much faster than MC and allows for extensive studies of dependences on pH, ionic strength, the type of distribution of H units in the shell-forming chains, etc., which would be impossible by MC. On the other hand, MC provides necessary details and hints how to interpret the angularly averaged functions.

The exaggerated sensitivity of SCF results to pH and ionic strength could be, according to our opinion, explained by the following arguments. In contrast to MC, the SCF approach does not strictly respect the connectivity and the self-avoiding character of individual chains. The electrostatic forces thus affect the behavior directly without any obstacles, and the ionization-mediated pH-dependent response is enhanced. The MC chains are strictly self-avoiding, and certain conformations cannot be achieved. As a result, the charges redistribute along annealed polyelectrolyte chains to minimize the Gibbs function, which

provides a certain feedback attenuating the effect of electrostatic forces on conformations.

Acknowledgment. The authors thank the Grant Agency of the Czech Republic (Grants 203/04/P117 and 203/07/0659), the Grant Agency of the Academy of Sciences of the Czech Republic (Grant IAA401110702), the Ministry of Education of the Czech Republic (long-term research plan MSM0021620857), the European Union (Marie Curie RTN, Grant 505027), the Meta-Center, CESNET, for the computer time, and Dr. Z. Tuzar for a beneficial discussion.

References and Notes

(1) Savic, R.; Eisenberg, A.; Maysinger, D. *J. Drug Targeting* **2006**, *14*, 343.
(2) Harada, A.; Kataoka, K. *Prog. Polym. Sci.* **2006**, *31*, 949.
(3) Yu, Y. S.; Eisenberg, A. *J. Am. Chem. Soc.* **1997**, *119*, 8383.
(4) Kiserow, D.; Prochazka, K.; Tuzar, Z.; Ramireddy, C.; Munk, P.; Webber, S. E. *Macromolecules* **1992**, *25*, 461.
(5) Azzam, T.; Eisenberg, A. *Angew. Chem., Int. Ed.* **2006**, *45*, 7443.
(6) Biggs, S.; Sakai, K.; Addison, T.; Schmid, A.; Armes, S. P.; Vamvakaki, M.; Butun, B.; Webber, G. *Adv. Mater.* **2007**, *19*, 247.
(7) Wang, D.; Yin, J.; Zhu, Z. Y.; Ge, Z. S.; Liu, H. W.; Armes, S. P.; Liu, S. Y. *Macromolecules* **2006**, *39*, 7378.
(8) Butun, V.; Liu, S.; Weaver, J. V. M.; Bories-Azeau, X.; Cai, Y.; Armes, S. P. *React. Funct. Polym.* **2006**, *66*, 157.
(9) Förster, S.; Abetz, V.; Müller, A. H. E. *Adv. Polym. Sci.* **2004**, *166*, 173.
(10) Pergushov, D. V.; Remizova, E. V.; Felthusen, J.; Zezin, A. B.; Müller, A. H. E.; Kabanov, V. A. *J. Phys. Chem. B* **2003**, *107*, 8093.
(11) O'Reilly, R. K.; Hawker, C. J.; Wooley, K. L. *Chem. Soc. Rev.* **2006**, *35*, 1068.
(12) Mitsukami, Y.; Hashidzume, A.; Yusa, S.; Morishima, Y.; Lowe, A. B.; McCormick, C. L. *Polymer* **2006**, *47*, 4333.
(13) Förster, S.; Hermsdorf, N.; Bottcher, C.; Lindner, P. *Macromolecules* **2002**, *35*, 4096.
(14) Birshtein, T. M.; Zhulina, E. B. *Polymer* **1989**, *30*, 170–177.
(15) Wijmans, C. M.; Zhulina, E. B. *Macromolecules* **1993**, *26*, 7214–7224.
(16) Zhulina, E. B.; Birshtein, T. M.; Borisov, O. V. *Macromolecules* **1995**, *28*, 1491–1499.
(17) Shusharina, N. P.; Linse, P.; Khokhlov, A. R. *Macromolecules* **2000**, *33*, 3892–3901.
(18) Borisov, O. V.; Daoud, M. *Macromolecules* **2001**, *34*, 8286–8293.
(19) Borisov, O. V.; Zhulina, E. B. *Macromolecules* **2003**, *36*, 10029–10036.
(20) Shusharina, N. P.; Zhulina, E. B.; Dobrynin, A. V.; Rubinstein, M. *Macromolecules* **2005**, *38*, 8870–8881.
(21) Susharina, N. P.; Linse, P.; Khokhlov, A. R. *Macromolecules* **2000**, *33*, 8488.
(22) Matějíček, P.; Podhájecká, K.; Humpolíčková, J.; Uhlík, F.; Jelínek, K.; Limpouchová, Z.; Procházka, K.; Špírková, M. *Macromolecules* **2004**, *37*, 10141–10154.
(23) Matějíček, P.; Uhlík, F.; Limpouchová, Z.; Procházka, K.; Tuzar, Z.; Webber, S. E. *Macromolecules* **2002**, *35*, 9487–9496.
(24) Jelínek, K.; Uhlík, F.; Limpouchová, Z.; Matějíček, P.; Procházka, K. *Collect. Czech. Chem. Commun.* **2006**, *71*, 756–768.
(25) Jelínek, K.; Uhlík, F.; Limpouchová, Z.; Procházka, K. *J. Phys. Chem. B* **2003**, *107*, 8241–8247.
(26) Jelínek, K.; Uhlík, F.; Limpouchová, Z.; Procházka, K. *Macromolecules* **2007**, *40*, 7656–7664.
(27) Uhlík, F.; Limpouchová, Z.; Jelínek, K.; Procházka, K. *J. Chem. Phys.* **2004**, *121*, 2367–2375.
(28) Uhlík, F.; Limpouchová, Z.; Jelínek, K.; Matějíček, P.; Humpolíčková, J.; Procházka, K.; Tuzar, Z.; Špírková, M.; Hof, M. *Mol. Simul.* **2003**, *29*, 665–660.
(29) Uhlík, F.; Limpouchová, Z.; Jelínek, K.; Procházka, *J. Chem. Phys.* **2003**, *118*, 1258–11264.
(30) Qin, A.; Tian, M.; Ramireddy, C.; Webber, S. E.; Munk, P.; Tuzar, Z. *Macromolecules* **1994**, *27*, 120–126.
(31) The PS−PMA micelles for experimental studies have been prepared by dialysis from 1,4-dioxane (80 vol %)−water mixture to aqueous buffers. The micellization equilibrium is reversible in this mixture, and it freezes during dialysis. In our recent studies, we have been using the association number based on the empirical scaling with the length of PS and PMA blocks. It yields 113 for symmetrical samples that we studied recently. Experimental values range from 100 to 120, slightly depending upon conditions (concentration, dialization velocity, etc.).
(32) Brandrup, J.; Immergut, E. H. *Polymer Handbook*, 2nd ed.; John Wiley and Sons: New York, 1967.
(33) Fleer, G. J.; Cohen Stuart, M. A.; Scheutjens, J. M. H. M.; Cosgrove, T.; Vincent, B. *Polymers at Interfaces*; Chapman and Hall: New York, 1993.
(34) Böhmer, M. R.; Evers, O. A.; Scheutjens, J. M. H. M. *Macromolecules* **1990**, *23*, 2288–2301.
(35) Israëls, R.; Leermakers, F. A. M.; Fleer, G. J. *Macromolecules* **1994**, *27*, 3087–3093.
(36) Wijmans, C. M.; Linse, P. *Langmuir* **1995**, *11*, 3748.
(37) Akinchina, A.; Shusharina, N. P.; Linse, P. *Langmuir* **2004**, *20*, 10351.
(38) van der Oever, J. M. P.; Leermakers, F. A. M.; Fleer, G. J. *Phys. Rev. E: Stat. Phys., Plasmas, Fluids, Relat.* **2002**, *65*, 41708.
(39) Schmid, F. *J. Phys.: Condens. Matter* **1998**, *10*, 8105–8138.
(40) Muller, M. *Macromolecules* **1998**, *31*, 9044–9057.
(41) Muller, M.; Binder, K. *Macromol. Symp.* **2000**, *159*, 97–104.
(42) Guo, L.; Ye, R. Q.; Ying, C. M.; Liu, H. L.; Hu, L. *Chin. J. Chem. Eng.* **2002**, *10*, 639–643.
(43) Reister, E.; Muller, M. *J. Chem. Phys.* **2003**, *118*, 8476–8488.
(44) Freire, J. J.; McBride, C. *Macromol. Theory Simul.* **2003**, *12*, 237–242.
(45) Kreer, T.; Metzger, S.; Muller, M.; Binder, K.; Baschnagel, J. *J. Chem. Phys.* **2004**, *120*, 4012–4023.
(46) Muller, M.; Smith, G. D. *J. Polym. Sci., Part B: Polym. Phys.* **2005**, *43*, 934–958.

MA071675Q